NASA TM-76971

NASA TECHNICAL MEMORANDUM NASA TM-76971

WALL INTERFERENCE CORRECTION IMPROVEMENTS FOR THE ONERA MAIN WINDTUNNELS

Xavier Vaucheret
ONERA

Translation of "Améliorations des calculs des effets de parois dans les souffleries industrièlles de l'ONERA", Office National d'Etudes et de Recherches Aérospatiales (ONERA), 92320 Châtillon (France), Fluid Dynamics Panel Specialists' Meeting on Wall Interference in Windtunnels held May 19-20, 1982, 12 pp.

NATIONAL AERONAUTICS AND SPACE ADMINISTRATION
WASHINGTON, D.C. 20546 AUGUST 1982

1. Report No.	2. Government Accession No.	3. Recipient's Catalog No.
NASA TM-76971		

4. Title and Subtitle	5. Report Date
WALL INTERFERENCE CORRECTION IMPROVEMENTS FOR THE ONERA MAIN WINDTUNNELS.	August 1982
	6. Performing Organization Code
7. Author(s) Xavier Vaucheret, ONERA, France	8. Performing Organization Report No.
	10. Work Unit No.
9. Performing Organization Name and Address Leo Kanner Associates, P.O. Box 5187 Redwood City, CA 94063	11. Contract or Grant No. NASW-3541
	13. Type of Report and Period Covered Translation
12. Sponsoring Agency Name and Address National Aeronautics and Space Administration, Washington, D.C. 20546	14. Sponsoring Agency Code

15. Supplementary Notes

Translation of "Améliorations des calculs des effets de parois dans les soufflerie industrièlles de l'ONERA", Office National d'Etudes et de Recherches Aérospatiales (ONERA), 93220 Châtillon (France), Fluid Dynamics Panel Specialists' Meeting on Wall Interference in Windtunnels held May 19-20, 1982, 12 pp.

16. Abstract This paper describes improved methods of calculating wall interference corrections for the ONERA large windtunnels. The mathematical description of the model and its sting support have become more sophisticated. An increasing number of singularities is used until an agreement between theoretical and experimental signatures of the model and sting on the walls of the closed test section is obtained. The singularity decentering effects are calculated when the model reaches large angles of attack. The porosity factor cartography on the perforated walls deduced from the measured signatures now replaces the reference tests previously carried out in larger tunnels. The porosity factors obtained from the blockage terms (signatures at zero lift) and from the lift terms are in good agreement. In each case (model + sting + test section), wall corrections are now determined, before the tests, as a function of the fundamental parameters M, CS, CZ. During the windtunnel tests, the corrections are quickly computed from these functions.

17. Key Words (Selected by Author(s))	18. Distribution Statement
	Unclassified-Unlimited

19. Security Classif. (of this report)	20. Security Classif. (of this page)	21. No. of Pages	22.
Unclassified	Unclassified		

N83-33908#
N-153,337

ABSTRACT

The methods used to compute wall interference corrections for the ONERA large windtunnels have been improved over the years. The mathematical description of the model and its sting support is more and more sophisticated; an increasing number of singularities is used until an agreement between theoretical and experimental signatures of the model and sting on the walls of the closed test section is obtained. The effect of the singularity displacement from the central position is calculated when the model reaches large angles of attack.

The porosity factor cartography on the perforated walls dededuced from the measured signatures now replaces the reference tests previously carried out in larger tunnels. The porosity factors obtained from the blockage terms (signatures at zero lift) and from the lift terms are in good agreement.

In each case (model + sting + test section) wall corrections are now determined, before the tests, as a function of the fundamental parameters M, CS, CZ. During the windtunnel tests, the corrections are quickly computed from these functions.

WALL INTERFERENCE CORRECTION IMPROVEMENTS FOR THE ONERA MAIN WINDTUNNELS

X. Vaucheret
ONERA

INTRODUCTION

/2*

The final closing discussion of the AGARD/FMP Symposium at Valloire in 1975 [1] confirmed the need to apply wall interference corrections to tests carried out in existing transonic windtunnels. The aim of these corrections is not to give the same results as those found during flight, because of the different Reynolds numbers, but to restore the speeds which have been modified by the presence of walls, both in magnitude and in direction. In this way, the results obtained using the same Reynolds for various windtunnels and for different model scales should be homogeneous. These types of comparison are a precious guide for checking the calculations of wall effects. Numerous comparative programs have thus become more and more sophisticated: this was the case with the tests carried out on standard ONERA models [2], or tests now being carried out on the F4 model within the framework of the GARTEUR group, made up of various organizations. Such is the constant concern of ONERA as it multiplies the comparisons of tests carried out in the various large three-dimensional S1, S2, S3MA and F1 windtunnels [3].

The investigation of wall effects has given rise to abundant literature since 1919. A study [4] of these effects on perforated walls has resulted in a list, although certainly incomplete, of 77 published references in 1977. At least as many works on slotted walls have been published. This large number of publications would lead one to think that the problem is solved. It appears, however, judging from the list of congresses held on the subject over the past ten years, that this is not the case. The AGARD/FDP congresses held in London in 1975 [5], Rhode Ste Genèse in 1976 [6], and

---

*Numbers in the margin indicate pagination in the original test.

Munich in 1980 [7] presented 27 reports on wall effects [8]. The last AIAA conference held this year at Williamsburg had a full session on wall effects [8]. We could, of course, mention this congress where 17 reports on wall effects only, will be given.

1 - RECENT IMPROVEMENTS IN WALL INTERFERENCE CALCULATIONS AT ONERA

The work on adaptive wall studies currently being conducted in ONERA two-dimensional windtunnels will not be considered here. This report will be concerned only with three-dimensional models in standard cylindrical test sections used for industrial tests. The reasons for conducting investigations to improve wall interference calculations in such cases may be classed in five groups:

-modern aircraft projects require greater accuracy, particularly for civil transonic transport aircraft
-larger angle of attack domains for modern fighters
-more powerful computers available for calculations
-measurements of signatures of model-sting combinations on the walls of test sections
-increased model sizes versus test sections offering a better representation of certain details, and a higher Reynolds number for testing.

Recent improvements in wall interference computations performed at ONERA will be described in this publication according to three viewpoints.

A) Improvement of the mathematical descriptions of models, in terms of both the number of singularities, and their location, particularly for cases of high angles of attack: actually because mechanisms are inserted in the test section to allow for models with higher angles of attack, these models become displaced from their central position. This report also describes the model supports, whereas, until now, models have been studied separately.

B) Utilisation of measurements of signatures of model-sting

combinations on the walls of test sections in order to, first, check out the validity of the mathematical description of model-sting combinations in the closed test section, and, second, to deduce the porosity factor cartographies on ventilated walls. This new method of procedure, therefore, makes it possible to omit the reference tests, such as testing in closed test sections, or in larger windtunnels, which have been used until now [9].

C) Reviewing the methods used to compute wall interference corrections: the tables of correction coefficients calculated in advance for a given test section, as a function of the numerous parameters, such as wall porosity, relative model span, wing sweep, span lift distribution, etc. will be discarded. The corrections are computed for each case (test section-model-sting) for a Mach grid, Cz, Cx, and the corrections are deduced in the form of polynomials as a function of these 3 parameters. This procedure offers a rapid method of computing the corrections for each test point.

2 - MATHEMATICAL DESCRIPTION OF THE MODELS AND STINGS /3

2.1 - Representing the Volumes

The volume of the model was initially [4] represented using a single doublet situated at the center of the model which is located in the standard position at the quadrant of the mean aerodynamic chord. Empirical coefficients were added to account for the fuselage slenderness, and the relative dimensions of the model in the test section. This made it possible to calculate the Mach number, normally assumed to be at the center of the model. Conversely, the volume blockage gradient is considered to be incorrect, where one singularity cannot account for the law of area. Moreover, the model signatures on the walls of the test section were too concentrated, and this led to the estimation of a premature blockage in the closed test section. After equipping the walls of the test sections with pressure pick-ups, it was found that the experimental signatures were noticeably different than the theoretical signatures.

For these various reasons, the fuselage of the models was represented by a set of doublets, the fuselage length is divided into N equal intervals for which the elementary volumes are calculated from the law of area together with their respective center of gravity. Each elementary volume is represented by a doublet situated at the center of gravity of the volume; the doublet intensity, proportional to the elementary volume, is assigned a term of compressiblity deduced from the corrected Mach number calculated in its position after several iterations. The doublets number N retained is that above which the signatures and corrected Mach distributions on the fuselage axis are not modified.

Figure 1 shows the signatures of a slenderness ellipsoid, in a closed test section, obtained with a description by 1, 2, 3, and 12 doublets. The signature becomes asymptotic after 12 doublets. After this number, and especially with a single doublet, the signatures are too concentrated and do not exhibit the stat' of spread obtained with a large enough number of doublets.

A simple rule, deduced from calculations for various ellipsoid slendernesses, consists of taking a number of equal or double doublets of the fuselage slenderness.

Figure 2 gives a comparison of the calculated and measured signatures of a large scale missile 5.3 meters long, obtained in a closed test section of the SIMA windtunnel 8 meters in diameter. In this case, the satisfactory agreement between these signatures is obtained with 30 doublets. The calculated signatures "customize" the model configuration quite well, as shown by the measurements given in the case of a single fuselage or of the full missile with nacelles and tail units. The signatures reflect the form of the law of area. The signatures calculated with a single doublet, given for reference, in a broken line, would be perfectly incorrect, because they are too concentrated and have a maximum Mach that is too high.

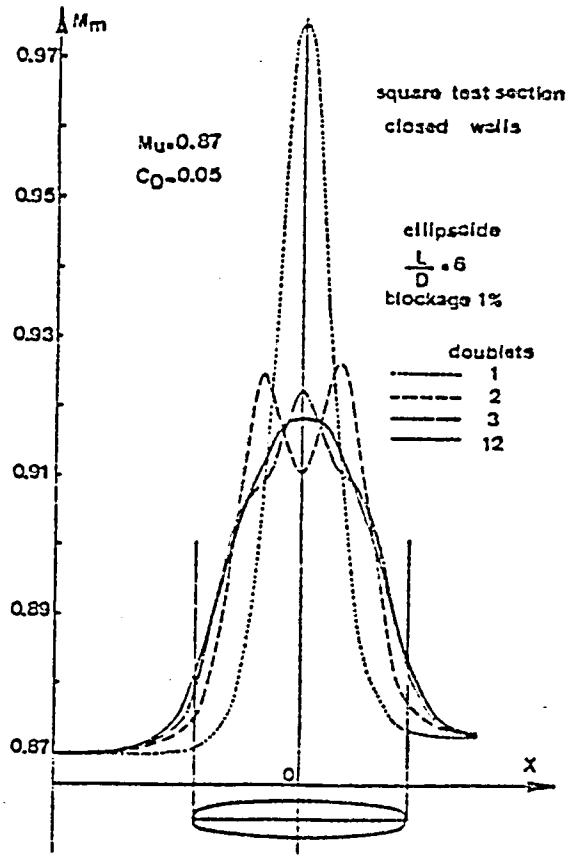

Fig. 1 - Effect of the number of doublets on the signature of an ellipsoid in a closed test section.

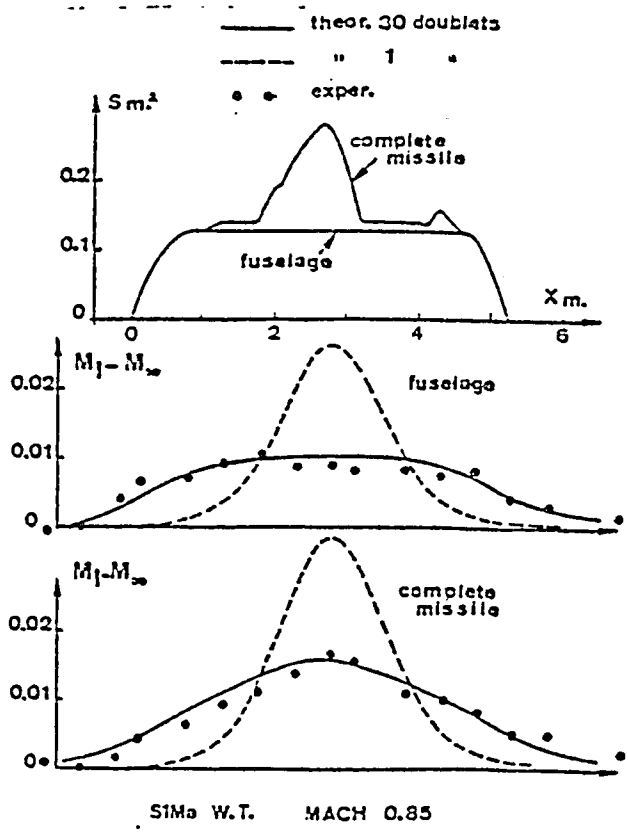

Fig. 2 - Theoretical and experimental signatures of a missile in a closed test section.

From this fact, the blockage limits of the model in the test section were obtained prematurely by the calculation (figure 3), whereas with a large enough number of doublets, the blockage is predicted at a Mach number exceeding about 0.02. The tests substantiate fairly well that the blockage appears only above Mach 0.9 for the complete missile. /4

The distribution of the corrected Mach number along the model axis is directly proportional to the local coefficients $\Omega_3[4]$ for a single doublet or with analogous coefficents Ω_{3z} for N doublets. Figure 4 gives, for different factors of reduced porosity $[\Omega,[4]$, the longitudinal distributions of coefficients Ω_3 and Ω_{3z} for 1

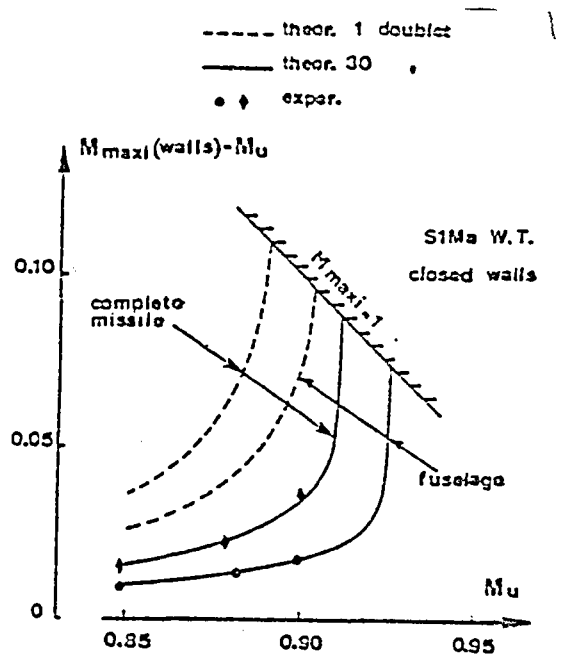

Fig. 3 - Prediction of the Mach blockage number in the closed test section.

and 20 doublets representing the slenderness ellipsoid 6 with 1% obstruction. With 20 doublets, the curves are always smaller. In this same figure, the Mach corrections (Mc - Mu), at the ellipsoid center, are also reduced by using the correct number of doublets.

It follows that the "Archimedean thrust" corrections, due to volume blockages, themselves directly related to the longitudinal gradients of the $\{\Omega_x\}$ coefficients, i.e. $\{\Omega'_x\}$ and $\{\Omega'_{xx}\}$ for 1 and N doublets, are modified (fig. 5). These ΔC_{x_s} corrections are therefore reduced to an absolute value (figure 5).

If we intuitively situated the previously considered single doublet at the center of this volume for the case of an ellipsoid, there would still be an unkown when a single doublet is used for a fuselage: its location. From this standpoint, the ΔC_{x_s} correction changed (figure 6), whereas with a set of the correct number of doublets, this correction stayed the same.

2.2 - Representing the Wake and the Separations /5

For the case of a fuselage, the wake blockage was calculated by using a source, situated at the center of the model, of intensity proportional to the theoretical drag coefficient. In recent calculations, the source may be placed at any location. The effect of the backward travel of the source from the center of the model at the base is shown in figure 7: it reduces the Mach corrections along the fuselage axis together with the level of the signatures

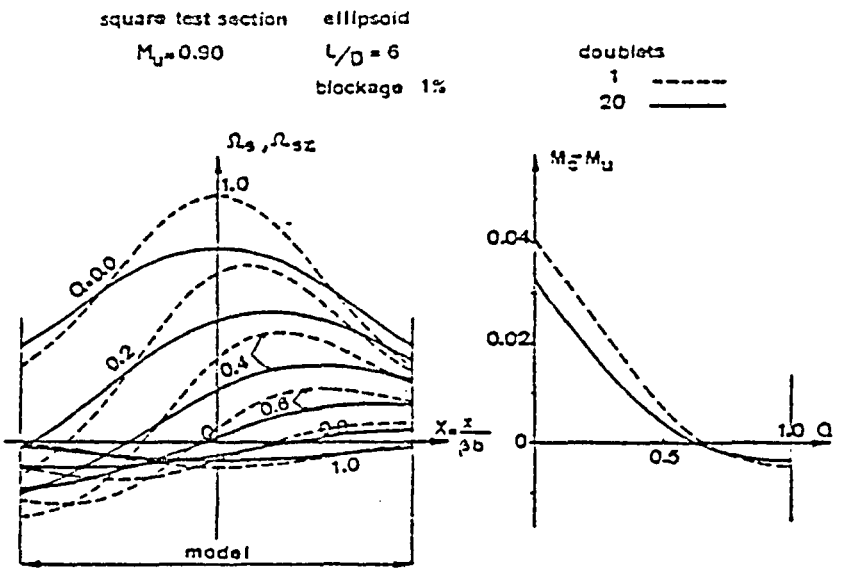

/4

Fig. 4 - Influence of the modeling of an ellipsoid on the Mach correction on ventilated walls.

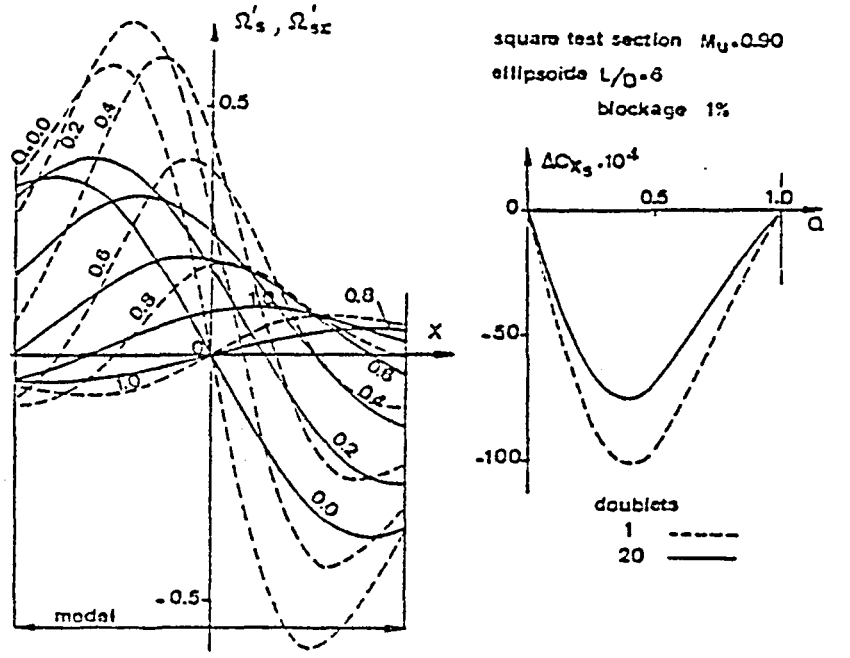

/5

Fig. 5 - Influence of the modeling of an ellipsoid on the buoyancy correction on ventilated walls.

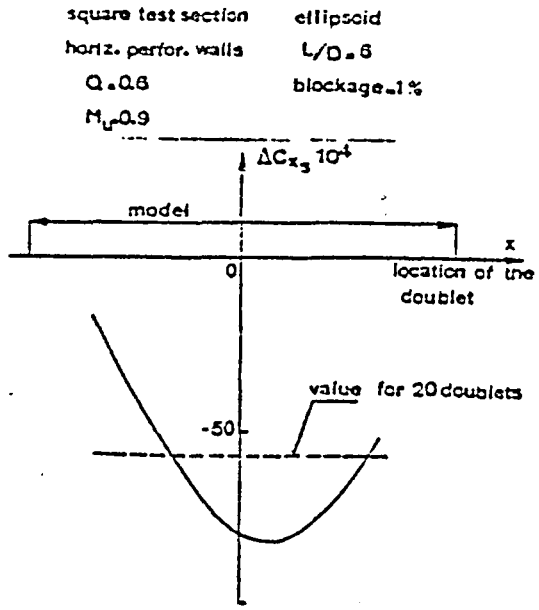

Fig. 6 - Influence of the doublet position on the buoyancy correction.

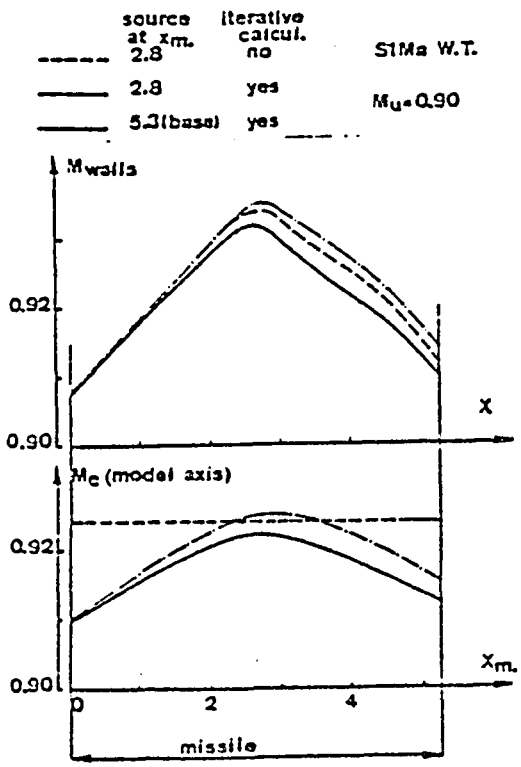

Fig. 7 - Influence of the position of the source and the calculation iterations on the signatures.

on the wall of the test section. It is therefore important to specify the location of the wake.

For the case of an aircraft model, the problem of the location and of the singularities used to represent the wake and the separations with large angles of attack is definitely more complex. The best models today have been proposed by HACKETT [9, 10].

It should be pointed out, as already mentioned in section 2.1, that the singularities used to represent the volumes and the wakes have weighted intensities by the compressibility term deduced from the Mach number corrected at the location of each singularity. This implies an iterative calculation: the number of iteration, of course, increases with the Mach number. Figure 7 illustrates the effect of the iterations for the case of the preceding missile at SIMA at Mach 0.90. The importance of these iterations is obvious on the calculation of blockage in the closed test section.

2.3 - Inclusion of the Sting Support

/6

Until now, the model has been described mathematically without its sting support. Figure 8 shows that for the case of a standard ONERA MS model [2] mounted on a straight sting in the transonic test section with closed configuration of the S3MA at Mach 0.83, the theoretical signatures at zero lift are different than the experimental signatures using 20 doublets to represent only the model. The difference becomes more significant toward downstream.

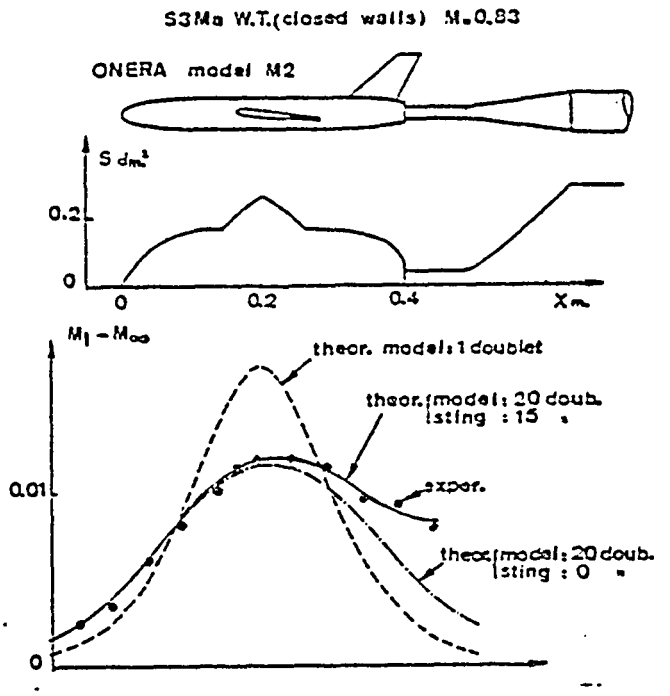

Fig. 8 - Model and Sting Signatures in a closed Test Section.

The modeling of the support using 15 doublets added to that of the model, made it possible to obtain an excellent agreement between the theoretical and experimental signatures, even outside the area occupied by the model. It is therefore important to account for the area requirement of the sting support, particularly because the sting areas often overshoot the model's partition.

The corrected Mach distributions, along the axis of the model, and proportional to the Ω_{sx}, coefficients, are given in figure 9. These are comparative effects of the interaction terms due to the wall effects (and not effects of the set of potentials due to the model being in an unlimited atmoshpere 'φ_m' and due to the 'φ_i' interactions. The blockage effects from the sting, downstream from the model, will have repercussions here in the entire area occupied by the model. This influence increases as the Mach decreases.

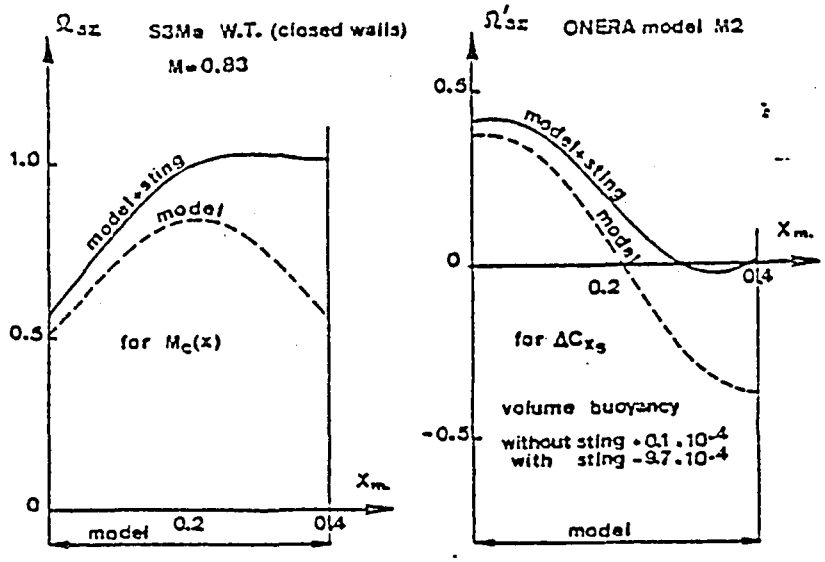

/7

Fig. 9 - Sting Effects on the Blockage Corrections

The derivative Ω'_{sx} of the preceding function $\Omega_{sx}(x)$ leads to the correction of the Archimedean thrust ΔC_{xs} induced by the blockage terms. Figure 9 shows the alternation of the $\Omega'_{sx}(x)$ curves. For the model only, this curve had an odd number, which leads to a correction ΔC_{xs} of practically zero. Conversely, the presence of the sting gives Ω'_{sx} which are almost always positive, except on the tail region. Consequently, the ΔC_{xs} correction is negative. The resulting error, by not taking the sting into consideration, is about 10.10^{-4} in drag, and is therfore large. The influence of the sting support on the model in an unlimited atmosphere (φ_∞ potential) should be added to this correction.

2.4 - Representing the Lift

/7

The lift is represented by a vortex sheet, without inclination, by accounting for the relative span, its sweep and the lift distribution on the span, if it is known [4]. Such a representation is appropriate for moderate angles of attack, but a few precautions should be taken for large angles of attack [3].

This modeling may be checked by noting the differences in the signatures on the high and low wall of the test section. Indeed, a comparison of the slopes on a point X, Y of the test section of

the curves showing the differences beween local Machs measured on the 2 slopes M_H M_B, as a function of C_z, is obtained using a δ^* coefficient analogous to the angle of attack correction coefficient δ [4].

Using the same standard ONERA M2 model, figure 10 gives a comparison of the theoretical and experimental δ^* coefficients which coincide satisfactorily for the cartography of the signatures on the two walls (curves at Y = 0 in the vertical plane of symmetry and at X = 0 in the transversal plane). This validates the modeling of the lift terms.

3 - DETERMINATION OF THE POROSITY FACTORS ON THE WALLS

3.1 - Signatures At Zero Lift

The mathematical representations of the models and stings are now sophisticated enough to obtain valid signatures in the closed test section. The problem of the boundary conditions on perforated walls, therefore, may now be handled.

Currently, the direct method which would consist of directly deducing the wall interference corrections from the theoretcial signatures is used only for 3D flow. An indirect method, by means of the porosity factor cartography on the walls, is the preferred method at the present time, because a basic objective searched for is to show whether the concept of uniform porosity should be abandoned or not.

The signatures are calculated as a function of a constant porosity factor on the walls. The theoretical signatures are reported on such a signature grid as a function of X and Q. Figure 11 thus gives the experimental signature, at zero lift, for the same ONERA M2 standard model mounted on a straight sting in a closed test section and in a test section with horizontal perforated walls. It may be seen that the latter signature coincides remarkably well with the experimental signature for Q = 0.2 which, /8

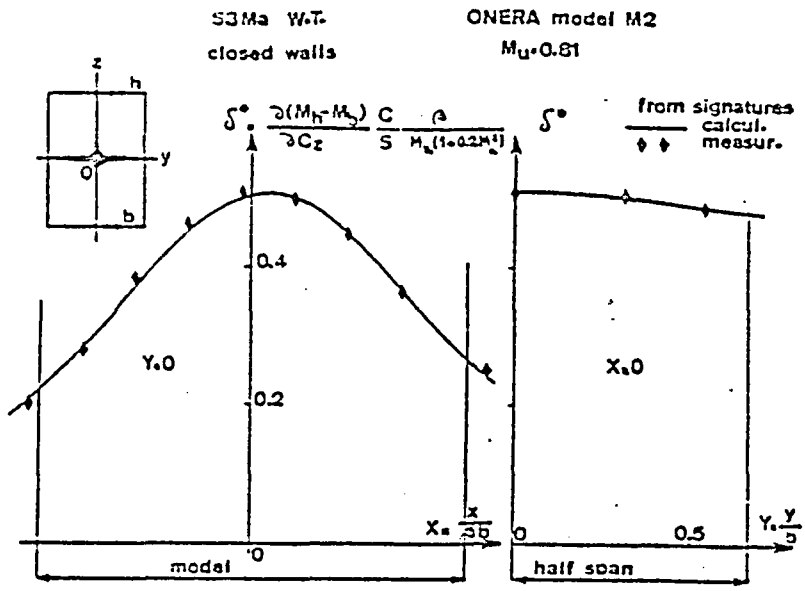

Fig. 10 - Comparison of Lift Terms Effects on the Signatures in a Closed Test Section.

/7

in this case, validates the concept of uniform porosity. Since this model is centered, the signatures used here at zero lift do not depend on the blockage terms. /8

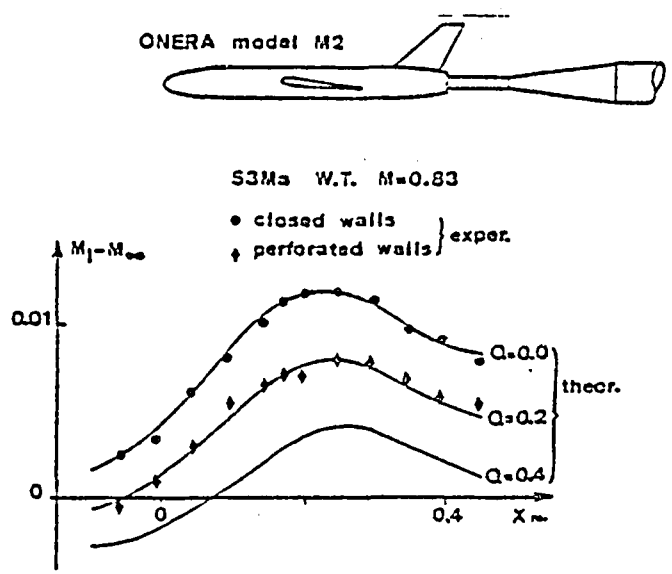

Fig. 11 - Determination of the Porosity Factors From the Signatures on Perforated Walls (Blockage Terms).

3.2 Signatures At Nonzero Lift

As indicated in paragraph 2.4, the difference between the signatures on the 2 high and low walls may be used to check the validity of the lift modelings. Once the validity is confirmed in the closed test section, it may be applied to porous walls to obtain the porosity factor cartography of the walls. Figure 12 illustrates this method for the case of the standard ONERA M2 model at S3MA in the perforated wall configuration.

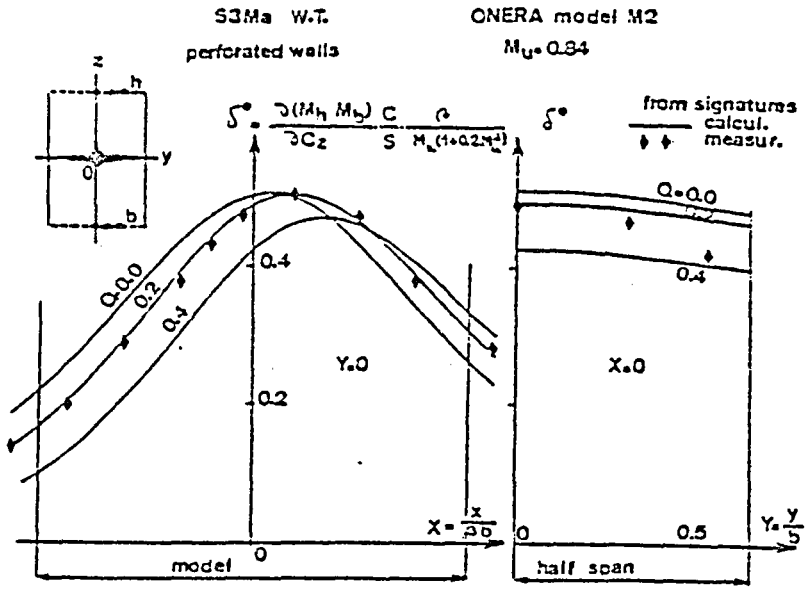

Fig. 12 - Determination of the Porosity Factors From the Signatures on Perforated Walls (Lift Terms).

In terms of the grid $\delta^*(x,y)$ calculated as a function of the porosity parameter $\underset{\sim}{Q}$ it is deduced that in the vertical plane of symmetry, a constant value of 0.2 is obtained for Q which agrees with the value found at zero lift (figure 11). It may therefore be noted that there is an identity of the porosity factors of the blockage (Cz zero) and lift terms. On the span, there is a slight increase of $\underset{\sim}{Q}$ from 0.2 to 0.35.

It now appears that the porosity factor cartographies may be deduced from signatures on walls and that the determination of porosity factors in reference tests performed in a closed test section or in a larger windtunnel may be abandoned. This new method has two incontestable advantages: first, supplementary reference tests are not needed, and second, the porosity requirements for every Mach and Reynolds range are defined, and this is often not possible during reference testing. However, this method requires a reading of the signatures which extends the testing time, although they can be limited to a number of Mach and angle of incidence points.

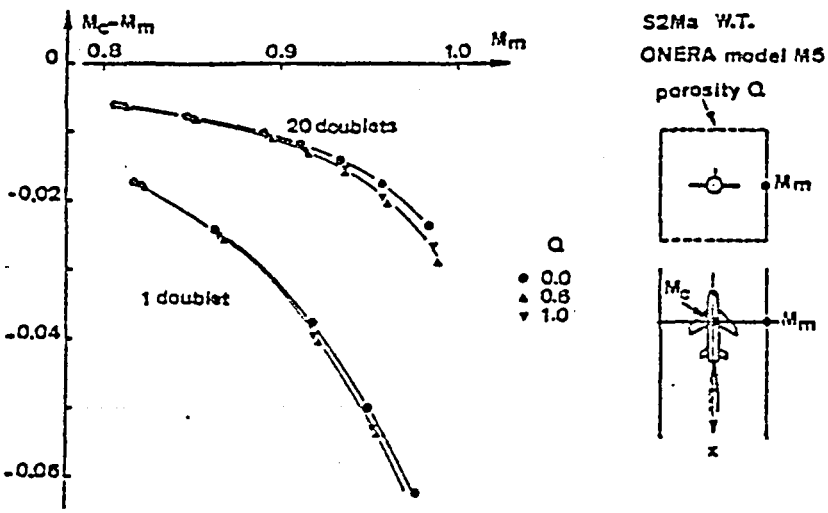

Figure 13 - Quick Method for Calculating the Mach Number.

3.3 - Rapid Method For Determining the Corrected Mach /9

Based on the formulations of the theoretical signatures on the model on the walls [4], an interesting method for determining the corrected Mach number has been obtained. This method consists of deducing the corrected Mach Mc from the theoretical Mach Mm on the entire wall perpendicular to the strut of the model (along the wing extension), whereas normally Mc is calculated from the theoretical Mach as far as possible upstream from the model to be free of its influence. In this case, however, Mc is calculated from the most interacting point of the model.

The incontestable advantage, as shown in figure 13, is to be able to do without knowledge of the wall porosity, because the correspondance between Mc and Mm is practically independent from the porosity factor on this particular point.

Only knowledge of the model's volume is needed. This rapid method requires only a very short computer time and makes it possible to conduct a test at a constant Mc. However, it requires a good modeling of the volumes of the models by taking into consideration the area requirements. Figure 13 thus shows that some 20 doublets are needed for forming a model of the mock-up. This figure illustrates the very small variation of the Mc - Mm correction as a function of the porosity factor for an ONERA M5 model in the S2MA windtunnel.

4 - THE EFFECT OF THE MODEL DISPLACEMENT FROM THE CENTRAL POSITION

In the mathematical representations described in paragraph 2, all of the singularities used are situated along the horizontal median plane of the test section. Such modelings are applicable to the case of models which are centered in the test section and for moderate angles of attack. In this particular case, the blockage terms result from the volume and wake singularities, and the angular flow corrections are deduced from the lift singularities.

If we now take models offset from their central position into consideration, or even models centered at a large angle of attack, we would have to take into consideration a set of singularities for any position in the test section, particularly outside the /10
horizontal median plane of the test section. The calculation of of the wall effects becomes complicated by quadratic interactions: accordingly, angular corrections are induced by volume and wake singularities and blockage corrections are deduced from the lift singularities. The importance of these terms increases with the singularity displacement from their central position; their effects are not negligible, and this is shown in the two examples given here.

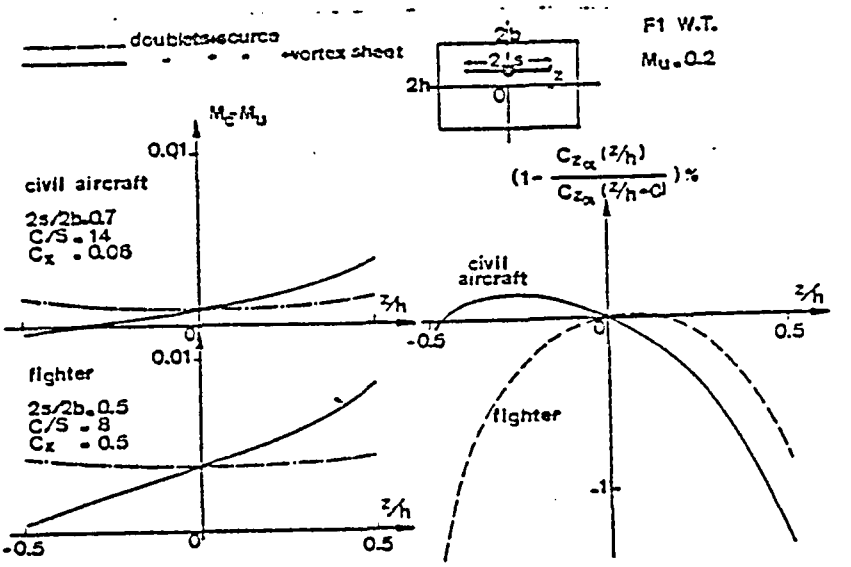

Fig. 14 - Influence of the Displacement From the Central Position of a Model on the Corrections in the Closed Test Section.

The first example refers to the new ONERA f1 windtunnel having a closed test section in the low speed range (figure 14). Two standard models, civil and fighter aircraft, of standard F1 size are examined. The Mach corrections $M_c - M_u$ are given as a function of the relative displacement from the center z/h of the models by taking into account, first, the volume and wake singularities, and, second, by adding the lift singularities; the significance of the latter terms is obvious. Figure 14 shows the lift gradient modifications resulting from the model's displacement from a central

position. The lift curve spread before corrections depends on the type of model: the order of the curves on an increasing gradient would therefore be: negative offset, zero is positive for civil aircraft, zero offset, negative then positive for the fighter.

The second example refers to a civil aircraft model in the S2MA transonic windtunnel with horizontal perforated walls & a reduced porosity factor σ close to 0.7. Figure 15 gives the Mach

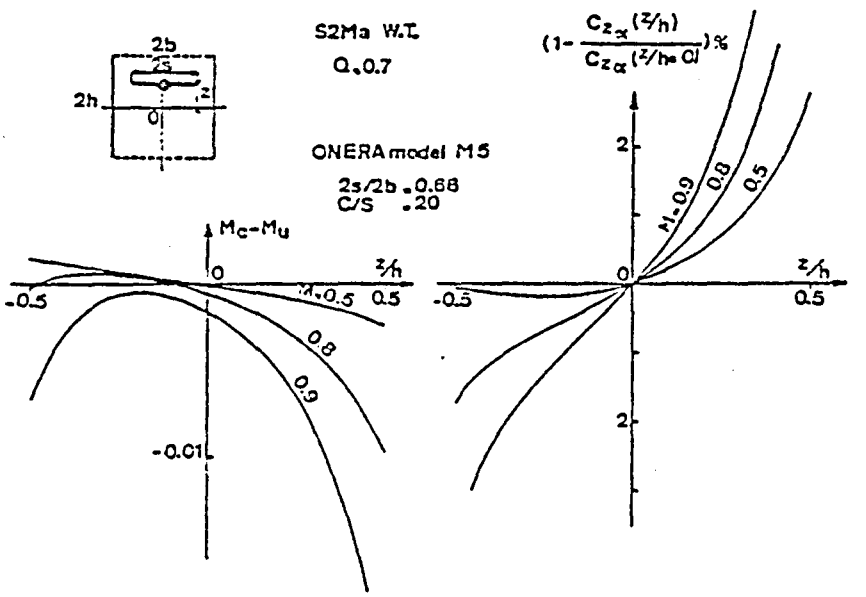

Fig. 15 -Influence of the Offsetting of a Model on the Corrections on Perforated Walls.

as a function of the offsetting at various test Mach, by including the wake and blockage singularities only, then by including the lift singularities: the curve dissymmetry increases with the Mach. The same applies to alterations of the lift gradient corrections.

A test result obtained on the standard ONERA M2 model in the S3MA windtunnel with perforated walls (figure 16), for 2 positions of the model: centered and positive decentering, shows that besides the variations of the lift gradients and the stabilities, the decentering modifies the angle of attack and the pitching moment at

zero lift. For the centered models, the classical calculations of corrections cannot explain such deviations. Conversely, by calculating with the decentered singularities makes it possible to predict: an angle of attack correction at zero Cz is deduced from decentered volume and wake singularities: figure 17 shows that this type of correction rapidly increases with the decentering and the Mach. The computer program for corrections with decentered singularities, in large enough numbers, is still being prepared.

5 - CALCULATIONS OF WALL INTERFERENCE CORRECTIONS /11

Owing to the increasing complexity of the calculations of wall interference corrections, resulting from more sophisticated modelings of the model-sting combinations, particularly for cases of decentering, it is no longer possible to construct tables of correction coefficients as done previously.

The corrections are computed for each test section, model, sting support, before a test: they require more and more sophisticated computer programmes. The corrections are defined for a grid of M, CX, CZ covering the test program and they are restored in the form of polynomials as a function of these three parameters. While the tests are being carried out, the corrections are computed for each test point from the previous polynomial, and are therefore clearly reduced and applicable to industrial testing programs.

CONCLUSIONS: FUTURE PROSPECTS

Figure 18 summarizes current improvements and those projected for the future. Regarding the mathematical modelings of the model-sting combinations placed in a test section, the transversal area requirements must still be defined to avoid concentrations of wing volumes, for example, on the model axis. Modelings of apex vorticities, nacelle jets and struts remain to be defined, as well as the means for deflecting the vortex sheets. It should be pointed

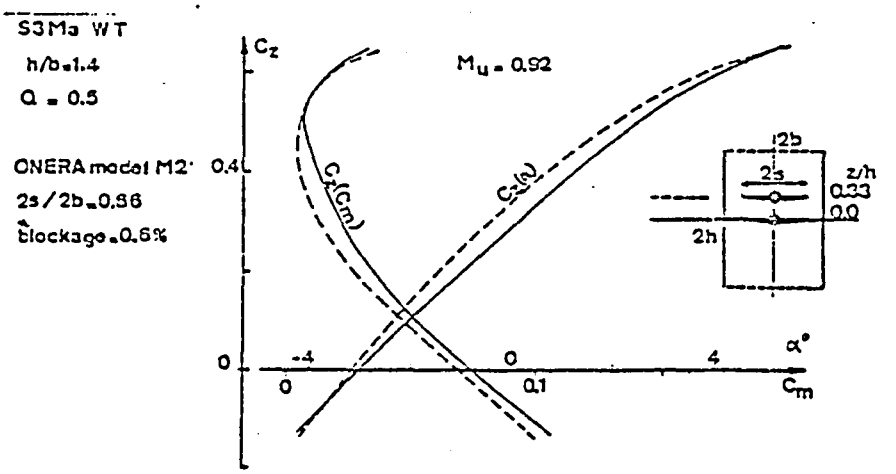

Fig. 16 - Test Results on Models With 2 Decenterings on Perforated Walls.

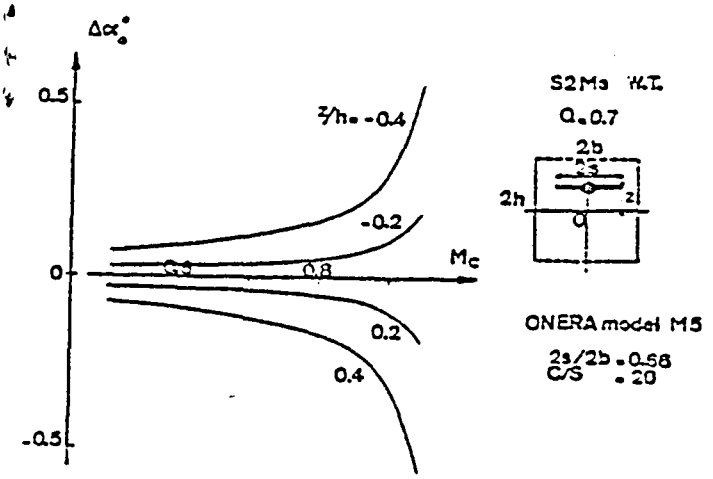

Fig. 17 - Inlfuence of the Decentering of a Model on the Angle of Attack at Zero Lift.

out that only the far fields are taken into consideration, and that consequently, only rudimentary, yet adequate, modelings are to be considered.

The indirect method of computing corrections, with determination of porosity factor cartography, will be discarded and replaced by a direct computer method using signatures, such as the one already used industrially for two-dimensional flow [11]. This method is based on the measurement of pressures on the walls of test sections, and the minimum number of pressures will first be determined for each type of correction in order to minimize the use of equipment on the walls, and therefore the data volume to be processed, and as a result, the length and cost of testing.

	SOLVED	TO SOLVE
2D	direct method : $sign._u$ → corrections	$sign._u$ troncature : α_o $sign._w$
3D	MATH. DESCRIPTION checking by $sign._u$ (closed walls) fuselage | doublets (x) sting | out of center (z) high α	wing volume doublets (y) vortex sheet incln. source for separ. region singularities for | apex vortex active jet strut
	CORRECTIONS indirect method : $sign._u \rightarrow Q(x,y,M) \rightarrow$ correct. special method → M_c , $\forall Q$	direct method : $sign._u \rightarrow$ correct. mini number of pressure points $sign._w$
	CONTROL reference tests	self adaptative walls large wind-tunnels

Figure 18 - Conclusions: Results Acquired, Future Studies.

The constant concern of windtunnel managers will result in multiplying the checks made of the corrections, by having recourse to every possible comparison of the results, within a given test section for various possible configurations, or between various windtunnels.

REFERENCES

1. "Flight/Ground Testing Facilities Correlation", AGARD CP 187 (Valloire, 1975).

2. Poisson-Quinton, Ph., Vaucheret X., "Predictions of the Aerodynamic Characteristics of an Aircraft Based on a Comparison of the Results Obtained on a Standard Model in Various Large Transonic Windtunnels", AGARD CP 242 (Paris, 1977).

3. Vaucheret, X., "Improvements Considered to Solve the Problems Found During Tests Performed on Models with Large Angles of Attack in Windtunnels.

4. Vaucheret, X., "Wall Corrections in Transonic Windtunnels-Equivalent Porosity Factor", ONERA PUBLICATION NO. 1977-3

5. "Windtunnel Design and Testing Techniques", AGARD CP 174 (London 1975).

6. "Numerical Methods and Windtunnel Testing", AGARD CP 210 (Rhode, Ste Génèse, 1976).

7. "Windtunnel Corrections for High Angle of Attack Models", AGARD Report No. 692 (Munich, 1980).

8. AIAA 12th Aerodynamic Testing Conference, Williamsburg, 1982.

9. Hackett, J., Wilsden, D., "Estimation of Windtunnel Blockage from Wall Pressure Signatures: A review of Recent Work at Lockeed", Georgia, AIAA Paper No. 78-828 (1978).

10. Hackett, J., "Living With Solid Walled Windtunnels", AIAA 12th Aerodynamic Testing Conference, AIAA 82-0583 (1982).

11. Capelier, C., Chevallier, J.P., Bouniol, F., "New Method for Correcting Flat Stream Wall Effects", La Recherche Aérospatiale, 1978-1.

End of Document